CHANDRASEKHAR, S. & MADHUSUDANA, N. V. (1970). *Mol. Cryst. Liquid Cryst.* **10**, 151.
CHATELAIN, P. (1955). *Bull. Soc. Franc. Minér. Crist.* **78**, 262.
CHEN, D. R., JAMES, P. G. & LUCKHURST, G. R. (1969). *Mol. Cryst. Liquid Cryst.* **8**, 71.
CHISTYAKOV, I. G. & CHAIKOVSKII, V. M. (1968). *Soviet Phys.-Cryst.* **12**, 770.
CHOW, L. C. & MARTIRE, D. E. (1969). *J. Phys. Chem.* **73**, 1127.
ELLIOT, G. & GIBSON, J. (1965). *Nature, Lond.* **205**, 995.
FOEX, M. G. (1933). *Trans. Faraday Soc.* **29**, 958.
GABRIELLI, I. & VERDINI, L. (1955). *Nuovo Cim.* **II**, 526.
GLARUM, S. H. & MARSHALL, J. H. (1966). *J. Chem. Phys.* **44**, 2884.
GRAY, G. W. (1962). *Molecular Structure and the Properties of Liquid Crystals.* London & New York: Academic Press.
GRAY, G. W. (1967). In *Liquid Crystals.* Edited by G. H. BROWN, G. J. DIENES & M. M. LABES, p. 129. New York & London: Gordon & Breach.
HEILMEIER, G. H. (1966). *J. Chem. Phys.* **44**, 644.
HOYER, W. A. & NOLLE, A. W. (1956). *J. Chem. Phys.* **24**, 803.
KAPUSTIN, A. P. (1970). Private communication.
KAPUSTIN, A. P. & BYKOVA, N. T. (1966). *Soviet Phys.-Cryst.* **11**, 297.
KAPUSTIN, A. P. & VISTIN, L. K. (1965). *Kristallografiya,* **10**, 118.
KOSTERIN, E. A. & CHISTYAKOV, I. G. (1968). *Soviet Phys.-Cryst.* **13**, 229.
LIPPMANN, H. (1957). *Ann Phys. Lpz.* **20**, 265.
MAIER, W. & SAUPE, A. (1958). *Z. Naturforsch.* **13***a*, 564.
MAIER, W. & SAUPE, A. (1959). *Z. Naturforsch.* **14***a*, 882.
MAIER, W. & SAUPE, A. (1960). *Z. Naturforsch.* **15***a*, 287.
MERWE, A. J. VAN DER (1966*a*). *Z. Phys.* **196**, 212.
MERWE, A. J. VAN DER (1966*b*). *Z. Phys.* **196**, 332.
ONSAGER, L. (1936). *J. Amer. Chem. Soc.* **58**, 1486.
SAKEVICH, N. M. (1967). *Izv. Vysshikh Uchebn. Zavedenii, Fiz.* **10**, 52.
SAUPE, A. (1968). *Angew. Chem. Intern. Ed.* **7**, 97.
SAUPE, A. & MAIER, W. (1961). *Z. Naturforsch.* **16***a*, 816.
SZIVESSY, G. (1925). *Z. Phys.* **34**, 475.
SZIVESSY, G. (1926). *Z. Phys.* **38**, 159.
WILLIAMS, R. (1963). *J. Chem. Phys.* **39**, 384.
ZADOC-KAHN, J. (1936). *Ann. Phys.* **11**, 455.
ZWETKOFF, V. (1942). *Acta Phys.-chim. URSS.* **16**, 132.

Acta Cryst. (1971). A27, 313

The Application of Non-Systematic Many-Beam Dynamic Effects to Structure-Factor Determination

BY J. GJØNNES AND R. HØIER

Department of Physics, University of Oslo, Norway

(*Received* 20 *July* 1970)

A method for utilizing non-systematic many-beam dynamic effects for determination of accurate relations between Fourier potentials is described. The effects which are used can be understood and described in terms of three-beam interactions; although quantitative evaluation is based on more interacting beams. The effects are most readily observed in Kikuchi patterns; experimental patterns from silicon are used as an example.

Introduction

It has been shown theoretically and experimentally by Uyeda and coworkers (Uyeda, 1968; Watanabe, Uyeda & Kogiso, 1968), that the contrast of the second-order Kikuchi line may vanish for a particular value of the acceleration voltage. This effect is due to variations in multiple-beam interactions with electron mass, and can be utilized to obtain very accurate relations between structure factors, as shown by Watanabe, Uyeda & Fukuhara (1968). The method does in a very simple way exploit dynamic effects for structure factor determination, but is limited to systematic reflexions and is dependent on high-voltage electron diffraction.

In a previous paper the present authors (Gjønnes & Høier, 1969) have studied enhancement and reduction of Kikuchi-line contrast, with particular emphasis on three-beam interactions. It was shown that a variety of contrast anomalies could be explained in terms of simple rules derived from three-beam considerations, *viz*, if the product $P=U_gU_hU_{g-h}$ of the Fourier potentials involved is positive, a weak beam, g, which is excited simultaneously with a strong beam, h, will be reduced in intensity relative to its two-beam value when the excitation error, ζ_h, of the strong beam is positive, and increased in intensity when ζ_h is negative. When P is negative, the effects are reversed with respect to the sign of ζ_h. Inclusion of more beams in the calculations will not as a rule alter the qualitative features. From this viewpoint the Uyeda–Watanabe effect can be seen as a special case of reduced intensity in a weak beam in a systematic, essentially three beam case, the excitation error of the strong beam being positive and constant along the Kikuchi line $2h$.

It was therefore found desirable to investigate intensity reduction in general, *i.e.* non-systematic, cases in order to find the conditions for complete vanishing of Kikuchi line contrast for a weak beam, and to see whether quantitative information about structure factors can be gained also from these cases. In addition we have studied the use of line splitting at Kikuchi line intersections, for structure factor determination. The methods are applied to patterns from silicon; appropriate corrections for the presence of further beams are introduced in the examples.

The three-beam case

It is assumed below that the contrast of a Kikuchi line is proportional to the width of the corresponding gap at the dispersion surface. Although no general proof for this has been presented, the available calculations (see Gjønnes & Høier, 1969), lend strong support to this assumption.

A set of coupled Kikuchi line intersections, T_o, T_h, T_g and T_m, is shown schematically in Fig. 1(*a*) where *e.g.* T_o is the area near the intersection between the two weak lines, $\bar{\mathbf{g}}$ and $\bar{\mathbf{m}}$, and a strong line, $\bar{\mathbf{h}}$.

Let us at first discuss the section L parallel to the strong line $\bar{\mathbf{h}}$ assuming that the contrast anomalies of the weak line **g** are due to coupling to the strong beam **h**, the coupling to **m** being negligible in this region. The product P is assumed to be positive; consequently, the three beam interaction leads to a reduction of the gap width between the two lower branches of the three beam dispersion surface relative to its two beam value. We shall now derive the condition, expressed by the excitation errors ζ_g and ζ_h, for which this gap width is reduced to zero as shown in Fig. 1(*b*). This corresponds to a double root of the third order secular equation for the *Anpassung* ξ:

$$\xi^3-\xi^2(\zeta_h+\zeta_g)+\xi[\zeta_h\zeta_g-U_g^2-U_h^2-U_{g-h}^2] \\ +[\zeta_h U_g^2+\zeta_g U_h^2-2U_g U_h U_{g-h}]=0\,.$$

Here and below the double wavevector $2\mathbf{k}$ is absorbed in ζ and ξ. By utilizing well known relations between the three roots and the coefficients of this equation one obtains the following expressions for the excitation errors:

$$\zeta_h=\frac{1}{2(U_g^2+\xi_o^2)}\,[2\xi_o(U_g^2-U_h^2)+2U_h U_g U_{g-h}+2\xi_o^3\mp\sqrt{z}] \tag{1}$$

$$\zeta_g=\frac{1}{2(U_h^2+\xi_o^2)}\,[-2\xi_o(U_g^2-U_h^2)+2U_h U_g U_{h-g}+2\xi_o^3\pm\sqrt{z}]$$

where ξ_o is the double root and

$$z=-4U_{g-h}^2\left[\xi_o+\frac{U_g U_h}{U_{g-h}}\right]^2(\xi_o^2+U_g^2+U_h^2)\,. \tag{2}$$

The only physically acceptable solutions are those giving real values of ζ which can be achieved for only one value of ξ_o, namely

$$\xi_o=-\frac{U_g U_h}{U_{g-h}}$$

in which case $z=0$

$$\zeta_g=\frac{U_g}{U_h}\cdot\frac{U_{g-h}^2-U_h^2}{U_{g-h}} \tag{3a}$$

and

$$\zeta_h=\frac{U_h}{U_g}\cdot\frac{U_{g-h}^2-U_g^2}{U_{g-h}}\,. \tag{3b}$$

It may be noticed that these values of the excitation errors change sign with the product P.

Equations (3*a*) and (3*b*) describe the condition for zero contrast. If this position can be located in the Kikuchi pattern, and measured with sufficient accuracy, they can therefore be used to obtain relations between structure factors.

The excitation error ζ_g is related to the position of the weak line at the point of vanishing contrast, whereas ζ_h is given by the position of this point along the weak line. One may thus expect the latter to be more useful, the displacement of the weak line from its geometrical position may be more conveniently utilized at the in-

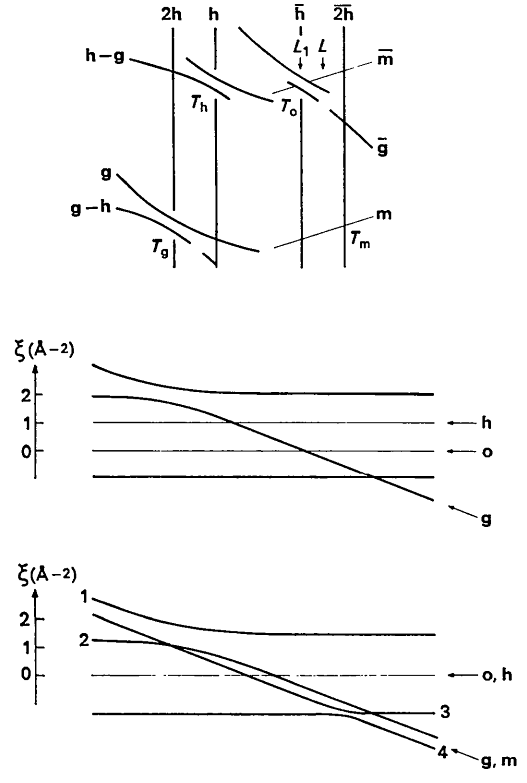

Fig. 1.(*a*) Schematic drawing of coupled Kikuchi line intersections, T_o, T_h, T_g and T_m, showing split lines and zero weak beam contrast outside a strong band (*b*) Calculated three-beam dispersion surface corresponding to section L in (*a*). $\mathbf{g}=\bar{5}7\bar{1}$, $\mathbf{h}=02\bar{2}$ and $\zeta_{02\bar{2}}=1{\cdot}03$ Å^{-2}. Si. 100 kV. (*c*) Calculated four-beam dispersion surface corresponding to section L_1 in (*a*). $\mathbf{g}=\bar{5}7\bar{1}$, $\mathbf{m}=\bar{5}15$ and $\mathbf{h}=02\bar{2}$. Si. 100 kV.

tersection with the strong line, as will be shown below. It is further seen from equations (3*a*) and (3*b*) that a relatively large value of $U_{\mathbf{g-h}}$ as compared with $U_{\mathbf{g}}$, is an advantage since it leads to a large value of $\zeta_{\mathbf{h}}$.

The three-beam dispersion surface corresponding to the section L_1 in Fig. 1(*a*) will be similar to Fig. 1(*b*) except that the two lines **o** and **h** will coincide, and the separation between the two horisontal branches will be equal to $2U_{\mathbf{h}}$. The intersections between these two branches and the weak beam sphere, **g**, define the positions of the split line **g** at the Kikuchi line intersection **g**, **h**. Assuming $U_{\mathbf{g}}$ and $U_{\mathbf{g-h}}$ to be weak compared with $U_{\mathbf{h}}$, one thus obtains for the separation of the two components of the split line

$$\zeta_{\mathbf{g}} = \pm U_{\mathbf{h}} \,. \qquad (4)$$

These excitation errors can be measured on the photographic plate. Consequently, equation (4) makes it possible to determine a strong Fourier potential without knowing any other potentials. Equation (4) includes, however, in most cases a systematic error as will be shown below.

A four-beam case

Even when the intersection between two lines includes a third intersecting line, as in Fig. 1(*a*), the contrast effects near the intersection can be explained qualitatively by three beam considerations. However, close to the point of intersection all beams should be taken into account. For the section L_1 in Fig. 1(*a*), *i.e.* $\zeta_{\mathbf{h}}=0$, the four beam case can be solved analytically as has been done by Fukuhara (1966), giving the four eigenvalues:

$$\xi_{1,2}=\tfrac{1}{2}(\zeta+U_{\mathbf{h}}+U_{\mathbf{g-m}} \pm \sqrt{(\zeta-U_{\mathbf{h}}+U_{\mathbf{g-m}})^2+4(U_{\mathbf{m}}+U_{\mathbf{g}})^2}) \qquad (5a)$$

$$\xi_{3,4}=\tfrac{1}{2}(\zeta-U_{\mathbf{h}}-U_{\mathbf{g-m}} \pm \sqrt{(\zeta+U_{\mathbf{h}}-U_{\mathbf{g-m}})^2+4(U_{\mathbf{m}}-U_{\mathbf{g}})^2}) \qquad (5b)$$

where ζ is equal to $\zeta_{\mathbf{g}}=\zeta_{\mathbf{m}}$.

The corresponding dispersion surface is shown in Fig. 1(*c*). We shall assume that the two maxima of the split line *g* originates from the two positions symmetrical around the kinematical position, where in this case the gaps $\xi_1-\xi_2$ and $\xi_3-\xi_4$ have minima. From equations (5*a*) and (5*b*) this is found to correspond to the excitation errors,

$$\zeta=\pm(U_{\mathbf{h}}-U_{\mathbf{g-m}}) \qquad (6)$$

which for a very weak coupling, $U_{\mathbf{g-m}}$, is seen to give equation (4). The assumption that only two of the branches contribute appreciably to the weak beam contrast is verified through four beam intensity calculations. The contributions from the other branches are small near the positions given by equation (6), and show a slow variation with the diffraction condition. The positions of maximum weak beam intensity are therefore shifted negligibly from the positions given by equation (6). Provided the potential, $U_{\mathbf{g-m}}$, is known, the strong potential can thus be determined by measuring the excitation errors on the plate.

Examples

An example of zero contrast is shown in Fig. 2 where the $\bar{4}22$ line in a pattern from Si is seen to vanish due to the interaction with $\bar{2}02$ and $\bar{2}20$; a geometry which was discussed already by Pfister (1953). In this case $\zeta_{\bar{4}22}=0$ according to equation (3) and

$$U_{220}=\sqrt{U_{422}(\zeta_{\bar{2}02}+U_{422})}$$

The $\bar{2}02$ excitation error was photometrically measured to be $\zeta_{\bar{2}02}=(2{\cdot}82\pm0{\cdot}06)$ Å^{-2} giving

$$U_{220}=(1{\cdot}42\pm0{\cdot}02)\ \text{Å}^{-2}$$

which is 4·5% above the tabulated value using a temperature factor $B=0{\cdot}45$.

To test whether many beam effects give rise to a shift in the position of zero contrast, up to nine beam calculations were performed, and the calculated position was found to be close to the measured one. A refinement on the 220 potential using the measured values of the excitation errors and assuming all potentials with higher indices to be known, gave the result:

$$U_{220}=(1{\cdot}362\pm0{\cdot}006)\ \text{Å}^{-2}$$

which corresponds to an atomic scattering factor for X-rays (Table 1) in accord with the tabulated value (*International Tables for X-ray Crystallography*, 1962). Calculations based on the second Bethe (1928) approximation resulted in a 220 Fourier potential 8% higher than the tabulated value.

Another example from Si is given in Fig. 3 showing the intersections between the line $\bar{5}7\bar{1}$, $02\bar{2}$ and $\bar{5}51$,$0\bar{2}2$. The position of zero contrast for the line $\bar{5}7\bar{1}$ does in

Table 1. 220 *structure factor in* Si *determined from many beam dynamic effects in Kikuchi line patterns* (100 kV)

	U_{220} (Å^{-2})					
Intersection	Equation (6)	2nd Bethe approx.	Equation (3)	9 beam	f_x^{calc} (Å^{-1})	f_x^{tab} (Å^{-1})
$\bar{4}22$, $\bar{2}02$		1·48	1·42 ± 0·02	1·362 ± 0·006	8·73 ± 0·03	8·71
$\bar{5}7\bar{1}$, $02\bar{2}$ (section *L*)		0·87	1·57 ± 0·20			
$\bar{5}7\bar{1}$, $02\bar{2}$ (section L_1)	1·40 ± 0·07					

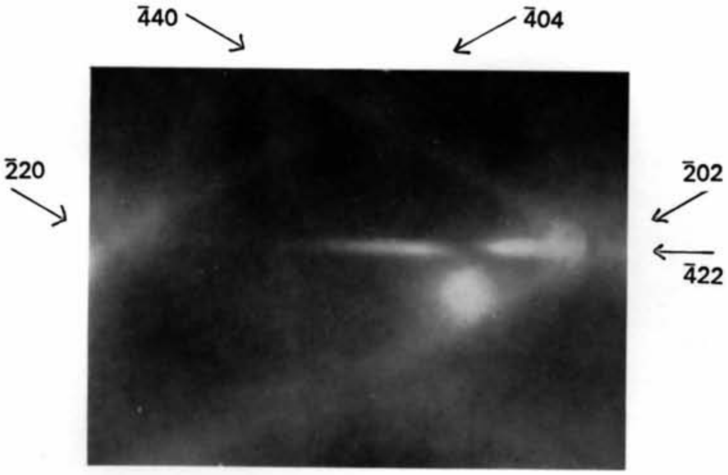

Fig. 2. Transmission Kikuchi pattern from Si showing zero $\bar{4}22$ contrast outside the $\bar{2}02$ and $\bar{2}20$ bands. 100 kV.

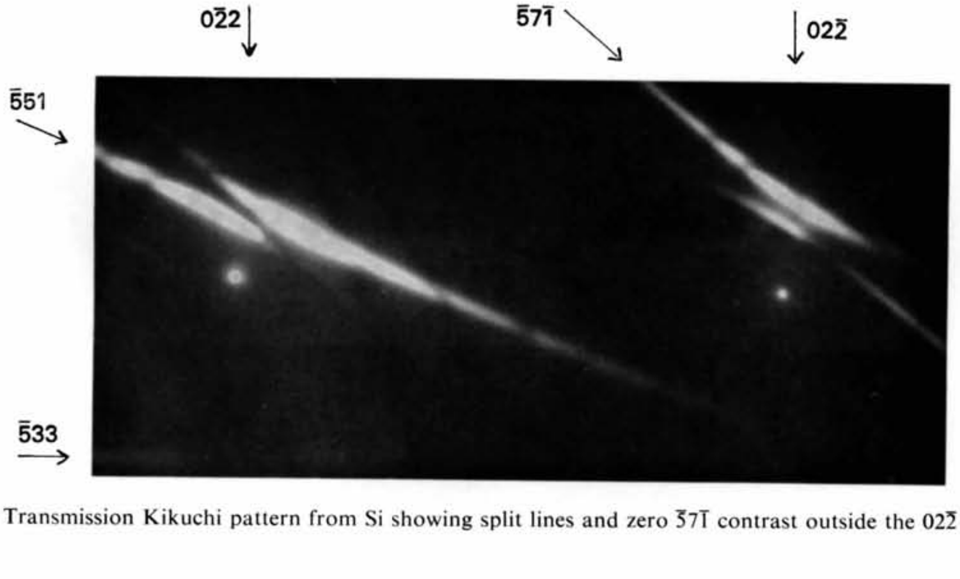

Fig. 3. Transmission Kikuchi pattern from Si showing split lines and zero $\bar{5}7\bar{1}$ contrast outside the $02\bar{2}$ band. 100 kV.

this case appear at a very small value of $\zeta_{02\bar{2}}$ resulting in a large uncertainty in the measurement of this quantity. From these measurements the 220 potential was determined to be

$$U_{220}=(1\cdot57\pm0\cdot20)\ \text{Å}^{-2}\,.$$

The second Bethe approximation gave a far too low value, as seen in Table 1.

The two maxima in the split $\bar{5}7\bar{1}$ line at the position $\zeta_{02\bar{2}}=0$ were measured to occur at

$$\zeta_{\bar{5}7\bar{1}}=\pm(1\cdot17\pm0\cdot07)\ \text{Å}^{-2}$$

which from equation (6) gives

$$U_{220}=(1\cdot40\pm0\cdot07)\ \text{Å}^{-2}$$

when the temperature factor is put equal to $B=0\cdot45$.

Conclusions

From the present study it can be concluded that non-systematic multiple beam dynamic effects in Kikuchi line patterns can be utilized for structure factor determination. These effects which are commonly observed at any acceleration voltage in weak lines near their intersections with strong bands or at equivalent positions in the pattern, can be localized and discussed by means of three-beam considerations. For quantitative structure factor determinations, however, corrections due to further beams have to be included in most cases. As distinct from the systematic many-beam case (Watanabe, Uyeda & Fukuhara, 1968) the second Bethe approximation was found to be inadequate for this purpose.

The accuracy of the present method will vary with the ratio between the structure factors involved and with the geometry of the interacting beams. Even in the more favourable cases the accuracy may be somewhat poorer than in the Uyeda–Watanabe method.

The main attraction by the present method is, of course, that one does not have to vary the acceleration voltage. It should also be pointed out that the use of non-systematic interactions introduces relations between other Fourier potentials than those belonging to a dense row in the reciprocal lattice.

The authors are grateful to Dr E. Nes for supplying the silicon samples.

References

Bethe, H. A. (1928). *Ann. Phys.* **87**, 55.
Fukuhara, A. (1966). *J. Phys. Soc. Japan*, **21**, 2645.
Gjønnes, J. & Høier, R. (1969). *Acta Cryst.* A**25**, 595.
International Tables for X-ray Crystallography (1962). Vol. III. Birmingham: Kynoch Press.
Pfister, H. (1953). *Ann. Phys.* **11**, 239.
Uyeda, R. (1968). *Acta Cryst.* A**24**, 175.
Watanabe, D., Uyeda, R. & Fukuhara, A. (1968). *Acta Cryst.* A**24**, 580.
Watanabe, D., Uyeda, R. & Kogiso, M. (1968). *Acta Cryst.* A**24**, 249.

Acta Cryst. (1971). A**27**, 316

Die Messung von Schallgeschwindigkeiten in optisch anisotropen Medien mit dem Schaefer–Bergmann-Verfahren

Von H. Küppers
Institut für Kristallographie der Universität zu Köln, Deutschland

(*Eingegangen am* 1. *April* 1970)

If the optical wave front is not normal to one of the principal axes of the indicatrix, diffraction of light in crystals, caused by ultrasound, is observed with maximum intensity when the incident beam is off the Bragg angle by an amount depending on double refraction. In a crystal plate of finite dimensions a standing ultrasonic wave also generates waves with propagation directions which are inclined to the normal of the plate, and interfere with the measurement of sound velocities by the improved Schaefer–Bergmann method. These difficulties are overcome by an appropriate choice of the angle of the incident light beam. Experiments with triclinic and trigonal crystals are reported. Formulae are derived for calculating the angles of incidence necessary for any measurements of sound velocities in crystals.

1. Einleitung

Das Schaefer–Bergmann-Verfahren (Beugung von Licht an Ultraschallwellen) wurde in den letzten Jahren zu einer Präzisionsmethode zur Messung von Schallgeschwindigkeiten und somit zur Bestimmung der elastischen Konstanten in durchsichtigen Festkörpern entwickelt (Haussühl, 1957). Der grösste Teil der bisher untersuchten Kristalle gehörte höhersymmetrischen Kristallklassen an. Die Messung der Geschwindigkeiten und die Berechnung der elastischen Konstanten erfolgt in diesem Fall am einfachsten, indem die Ge-